Estimating exhumation using experimental compaction trends and rock physics relations, with continuation into analysis of source and reservoir rocks: Central North Sea, offshore Norway

Jørgen André Hansen[*,1], *Honore Dzekamelive Yenwongfai*[1,2], *Manzar Fawad*[1] *and Nazmul Haque Mondol*[1,3]
[1]*University of Oslo,* [2]*Statoil ASA,* [3]*Norwegian Geotechnical Institute*

Summary

We present a quantitative estimate of exhumation in the Central North Sea by examining depth trends of velocity and density data compared to experimental compaction trends. Additionally, seismic inversion and attribute application from the study area is shown as an example of the connection to future work on quantitative analysis of source and reservoir rocks. Rock physics relations are demonstrated to be important for all parts of the study.

Introduction

Cenozoic exhumation affecting the Norwegian Continental Shelf (NCS) is well established and has been described in various publications over the last decades (e.g. Doré and Jensen, 1996; Hansen, 1996; Riis, 1996; Baig et al., 2016). The exhumation encompasses all three petroleum provinces (e.g. North Sea, Norwegian Sea and Barents Sea) along the NCS. The presented estimates of the magnitude of uplift and erosion for a given area often vary substantially with methods employed in the study. We present here an attempted refinement of the exhumation estimates of the Central North Sea (Fig. 1). The estimated exhumation is based on compaction trends of well log data (87 exploration wells within the indicated study area) and experimentally derived normal compaction trend (NCT). As seen in Figure 1, the study area is relatively less explored (lower density of wells) and has less exploration success compared to the Viking Graben (further north of the study area). A second look at previously overlooked areas can give potential for finding more oil and gas in the less explored Central North Sea. This study is meant to serve as important input for further work on both reservoir and source rocks in the area.

Methods

Firstly, shale volume was estimated by calculating the gamma ray index based on the interpretation of gamma ray values representing clean sand and pure shale, and correcting after Equation 1 (Clavier et al. 1971). Data estimated to represent mainly shaly lithologies ($V_{sh} > 0.5$) were used in further analysis.

$$V_{sh} = 1.7 - [(3.38 - (I_{GR} + 0.7)^2]^{1/2} \qquad \text{Eq. 1}$$

The exhumation can be estimated by comparing velocity-depth and density-depth trends to NCT established from experimental compaction of 50:50 silt-clay mixtures.

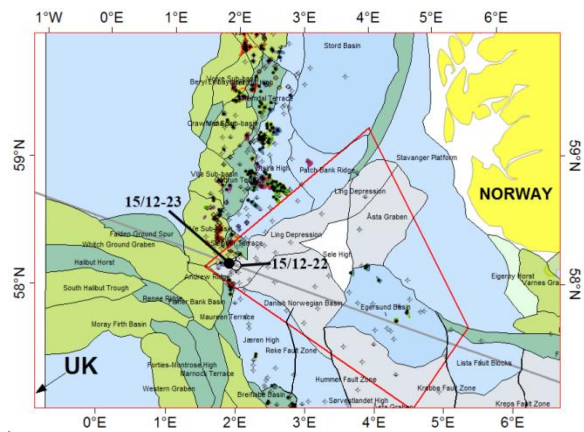

Figure 1: Overview of study area and structural elements (source: NPD FactMaps). Exploration wells and seismic line are marked.

The chosen NCT represents mechanical compaction of 50:50 kaolinite-silt (Mondol 2009) aggregates, which is shown to be a good model for representing shaly lithologies present on the NCS. A suitable depth shift (i.e. representing exhumation) is then approximated (where required) to obtain a good match between the well log data and the NCT. Equally important, the transition zone depth (change from the mechanical to chemical compaction domain) can be interpreted based on sudden increases in V_p and/or apparent deviations from the compaction trend. This is explained by a stiffening of rocks due to cementation, which occurs initially at 70-80^{o}C in mudstones, corresponding to ~2000-2500 m (e.g. Bjørlykke, 2015). Where measurements of shear velocity (V_s) are available, identification of the transition zone can be aided by crossplots of shear modulus (μ) versus density (ρ), as stiffening of the rock corresponds to increased values of μ (Storvoll and Brevik, 2008). A value of exhumation could subsequently be assigned to each well location, and used to make an exhumation map through a simple convergent interpolation algorithm.

Post-stack inversion for P-impedance was done on a 2D seismic line crossing two exploration wells in the study area (Fig.1). A strata model based on three key seismic horizons and well data from the two wells was used as a low frequency model for the impedance variations. Synthetic seismograms from the well log data were created using a statistical wavelet extracted from the seismic data, which was a zero phase wavelet with a dominant frequency of 20 Hz. The Emerge module of the Hampson-Russell software was used for training and application of a relation between the inversion and shear modulus with an error of 2.782 and a correlation of 0.7917. Due to a limited dataset with post-stack 2D data and a thick investigation interval, only one parameter was used to get an approximate representation of shear modulus.

Results

An example of a well showing signs of no exhumation is shown in a crossplot of P-velocity versus depth in Figure 2a. As the shallow data at present depth (below sea floor - BSF) shows good correlation with the experimental compaction curve, no depth correction is required and the rocks are assumed to be at their maximum burial. The transition zone can be inferred to be at around 2250 m based on a beginning deviation in the velocity data from the compaction trend, which is supported by examining the μ-ρ plot color coded by temperature in Figure 2b. A trend change or "kink" in the data towards increasing values of shear modulus with depth is assumed to represent the onset of chemical compaction (approximately >80^{o}C in this case based on present temperature gradient from BHT). An additional observation is that data from a source rock interval (which is indicated by the color code to be at temperatures between 90-100^{o}C) shows behavior similar to mudstones in the mechanical compaction domain, i.e. deviating from other rocks at similar temperature/depth.

Figure 3 shows estimation of exhumation in a well closer to the source of upliftment, where there is a clear discrepancy between the data and the compaction curve. By applying a depth shift of 250 m, we observe a good agreement with the reference trend and a more realistic temperature-depth relation. A second observation for this plot is related to clay mineralogy and pressure effects. We can see that smectite-rich mudstones (with possible overpressure) in the Hordaland Group do not conform to the reference compaction trend, as the compaction curve is based on experiments with larger clay minerals and silt. An inverted behavior of velocity with depth makes data from this region less suitable for predicting exhumation, which must be taken into consideration where the shallower sections are absent or eroded. The underlying Rogaland Group (with different mineralogical composition) displays a good fit with the compaction curve, indicating that chemical compaction has not affected rocks in this well at less than ~2400 m. Data from deeper intervals display high velocity values as expected, with the exception of a source rock interval of the Viking Group. The exhumation map resulting from this study is shown in Figure 4.

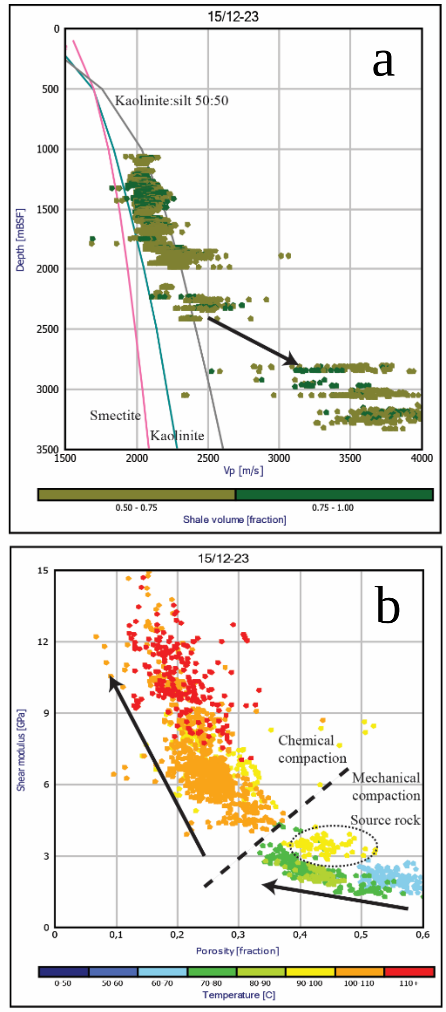

Figure 2: a) P-velocity versus depth BSF, data with $V_{sh} > 0.5$. The arrow indicates a distinct difference in V_p, i.e. transition zone. Compaction trends in figure 2a are from Mondol et al. (2007) and Mondol (2009). b) Porosity versus shear modulus plot, color coded by temperature.

An increase in exhumation towards the east and north-east can be observed, with values up to more than 1000 m in the margins of the study area. Due to the use of data in well locations exclusively when creating this map, we observe some mapping features (circular contours) and take note of a much higher density of wells in certain areas. The present day temperature gradient acquired from the bottom hole temperature (BHT) from the well data is highly variable in this region, which is likely an influence of both uplift and/or proximity to extensive salt structures. Equivalent maps of transition zone depth were created for present burial and assumed maximum burial, which provide a second quality control of possible unlikely exhumation values if the transition zone depth disagrees considerably from the expectation.

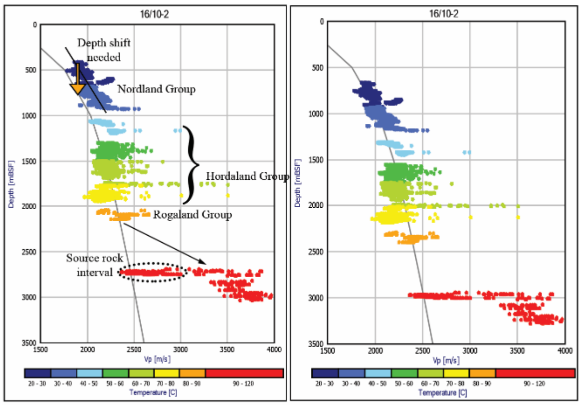

Figure 3: Velocity versus depth with data from a well indicating exhumation of ~250 m, based on the trend in the shallow data and temperature color coding. The arrow indicates a distinct difference in V_p, i.e. transition zone.

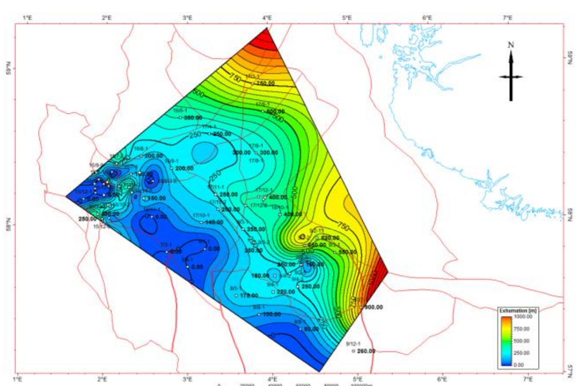

Figure 4: Exhumation map of the study area. Control points are marked by squares and with corresponding exhumation value.

A low frequency strata model, inversion analysis and final inversion for a seismic 2D line intersecting two wells in the area are shown in Figure 5 (a, b and c, respectively). This process was used as a first pass in an attempt look for similar features as described above regarding transition zone and source rocks. In the upper interval marked at the top by the Rogaland Formation horizon can be seen to have moderately low impedances indicated by yellow colors (Fig. 5c). A thick, high impedance chalk layer is seen below in purple to blue colors, followed by intermediate impedances indicated below the Cromer Knoll Group marker. The inversion analysis (Fig. 5b) indicates that the modeled P-impedance closely follows the low frequency model and has a reasonable correlation with the log-derived P-impedance values.

Computed shear modulus from the inversion is shown in Figure 6. As only one parameter was used in training the data, the result is similar to the P-impedance inversion, but some areas are more accentuated. Firstly, with regard to the transition from mechanical to chemical compaction, the interval between top Rogaland Group and top Chalk (Shetland Group) was examined. Somewhat higher values of μ are seen around well 15/12-23 (up to ~6 GPa below the uppermost layer, light green to yellowish color) than around well 15/12-22 on the right (~3 to 4 GPa, dark green to light green colors). The transition between the wells appears gradual and to be related mainly to depth rather than follow the geometry of the sedimentary layers. As described above in relation to Figure 2, the transition zone is expected to be approximately at this depth level, which is assumed to lead to stiffening of the mudstones and increased shear strength.

A second point of interest is the yellow-green low μ (and impedance) layer below the Viking Group marker. This is visible at both well locations and can be followed approximately across the section in Figure 6, indicating that the different properties of the source rock interval is detected by the current method to a certain degree. As the top of a source rock interval is characterized by significantly lower acoustic impedance than similar mudstones without organic content (Løseth et al. 2011) and a characteristic AVO signature (e.g. Gading et al. 2012), the inversion process can be used to highlight variability in source rocks between wells which is not necessarily visible in the conventional seismic image. The challenge is to find the inversion attribute(s) that have a good correlation to geological properties that are relevant to describe the source rock. Examples of these are, in addition to the amount of organic content, changes in elastic parameters due to maturation, generation and expulsion of hydrocarbons. Source rocks in areas buried to depths close to the oil window, or in areas which have been uplifted, could have a local lateral variation in maturity and consequently potential local generation of hydrocarbons. For this purpose, knowledge of uplift magnitude, temperature gradient (and preferably an idea of the earlier temperature regime) and cementation depth can be valuable input. Similarly, the same approach could be applied to potential reservoir units at depths approximately corresponding to temperatures initiating cementation, where burial differences over relatively short distances could result in different reservoir quality and fluid sensitivity on AVO signature (e.g Avseth et al. 2009).

Conclusions

A technique for estimating exhumation based on experimental compaction trends and well log data has been utilized over a large area in the Central North Sea. The technique is easily applied to common well measurement data, as long as the correct considerations are taken with regard to variations in clay mineralogy and overpressure. Furthermore, the goal is to transfer this knowledge into future studies involving quantitative analysis of source and reservoir rocks in the area. An example is shown by utilizing an inversion and application of an attribute to the seismic section.

Acknowledgements

This study was carried out under the ReSource project, an R&D collaboration between the University of Oslo and Eni Norge. We extend our thanks to DISKOS for providing data and Eni Norge for funding.

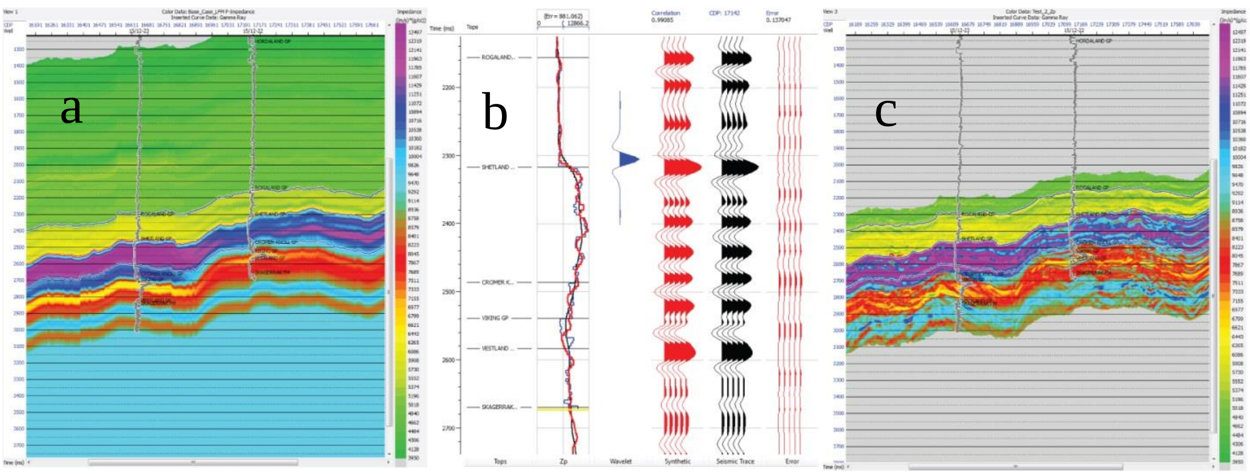

Figure 5: Low frequency strata model (a), inversion analysis (b) and P-impedance inversion in target interval (c).

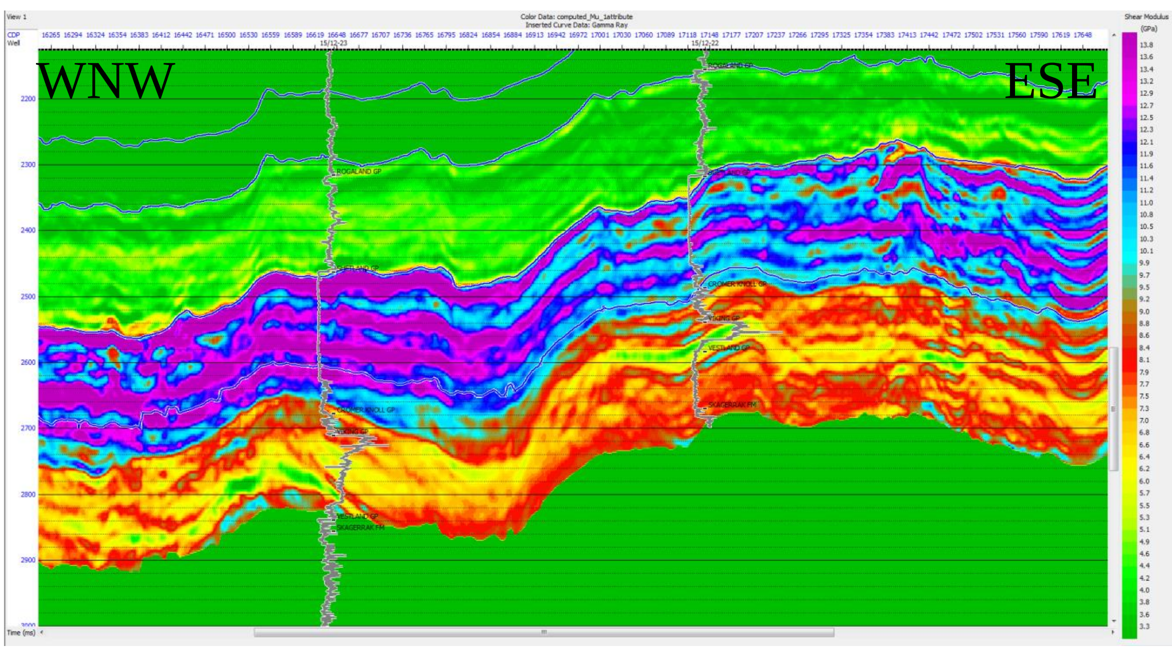

Figure 6: Application of single attribute regression (sqrt (impedance inversion)) for shear modulus. Correlation = 0.7968, average error = 2.74 GPa. Gamma ray logs are inset at the well locations.

EDITED REFERENCES

Note: This reference list is a copyedited version of the reference list submitted by the author. Reference lists for the 2017 SEG Technical Program Expanded Abstracts have been copyedited so that references provided with the online metadata for each paper will achieve a high degree of linking to cited sources that appear on the Web.

REFERENCES

Avseth, P., A. Jørstad, A.-J. van Wijngaarden, and Mavko G., 2009. Rock physics estimation of cement volume, sorting, and net-to-gross in North Sea sandstones: The Leading Edge, **28**, 98–108, https://doi.org/10.1190/1.3064154.

Baig, I., J. I. Faleide, J. Jahren, and N. H. Mondol, 2016, Cenozoic exhumation on the southwestern Barents Shelf: Estimates and uncertainties constrained from compaction and thermal maturity analyses: Marine and Petroleum Geology, **73**, 105–130, https://doi.org/10.1016/j.marpetgeo.2016.02.024.

Bjørlykke, K., 2015, Compaction of sedimentary rocks: Shales, sandstones and carbonates, *in* K. Bjørlykke, ed., Petroleum geoscience: From sedimentary environments to rock physics (2nd ed.): Springer-Verlag Berlin Heidelberg, 351–360.

Clavier, C., W. Hoyle, and D. Meunier, 1971, Quantitative interpretation of thermal neutron decay time logs: Part I. Fundamentals and techniques: Journal of Petroleum Technology, **23**, 743–755, https://doi.org/10.2118/2658-A-PA.

Doré, A. G. and L. N. Jensen, 1996, The impact of late Cenozoic uplift and erosion on hydrocarbon exploration: Offshore Norway and some other uplifted basins: Global and Planetary Change, **12**, 415–436, https://doi.org/10.1016/0921-8181(95)00031-3.

Gading, M., L. Wensaas, and H. Løseth, 2012, Source rocks from seismic, Part-2 — Applications: 74th Annual International Conference and Exhibition, EAGE, Extended Abstracts, http://doi.org/10.3997/2214-4609.20148770.

Hansen, S., 1996, Quantification of net uplift and erosion on the Norwegian Shelf south of 66°N from sonic transit times of shale: Norsk Geologisk Tidsskrift, **76**, 245–252.

Løseth, H., L. Wensaas, M. Gading, K. Duffaut, and M. Springer, 2011, Can hydrocarbon source rocks be identified on seismic data?: Geology, **39**, 1167–1170, http://doi.org/10.1130/G32328.1.

Mondol, N. H., 2009, Porosity and permeability development in mechanically compacted silt-kaolinite mixtures: 79th Annual International Meeting, SEG, Expanded Abstracts, 2139–2143, https://doi.org/10.1190/1.3255280.

Mondol, N. H., K. Bjørlykke, J. Jahren, and K. Høeg, 2007, Experimental mechanical compaction of clay mineral aggregates — Changes in physical properties of mudstones during burial: Marine and Petroleum Geology, **24**, 289–311, https://doi.org/10.1016/j.marpetgeo.2007.03.006.

NPD FactMaps, 2017, Norwegian Petroleum Directorate, Available: http://gis.npd.no/factmaps/html_20/ [Accessed 15. March 2017].

Riis, F., 1996, Quantification of Cenozoic vertical movements of Scandinavia by correlation of morphological surfaces with offshore data: Global and Planetary Change, **12**, 331–357, https://doi.org/10.1016/0921-8181(95)00027-5.

Storvoll, V., and I. Brevik, 2008, Identifying time, temperature, and mineralogical effects on chemical compaction in shales by rock physics relations: The Leading Edge, **27**, 750–756, https://doi.org/10.1190/1.2944160.